Magneto-Thermoelastic Analysis of Ferromagnetic Plate Exposed to High-Frequency Induction Heater

B. B. Balpande* [iD] and G. D. Kedar [iD]

Department of Mathematics, RTM Nagpur University, Nagpur 440033, Maharashtra, India

*Corresponding author: bhushanbalpande@rediffmail.com

Abstract. A mathematical model for studying the consequences of a moving high-frequency induction heater on a ferromagnetic plate material was presented in the context of Maxwell's equation. Conducting currents are generated when the material is exposed to electromagnetic fields operating at high frequency. The losses due to conducting currents and the hysteresis effect are summed and considered as the total heat loss of the problem. The expressions for heat losses, temperature field, elastic field, and magnetic field are obtained across the plate material in the context of Maxwell's equations and Ohm's law and are solved using the double finite Fourier sine and Marchi-Fasulo integral transforms. Lastly, the effects of the plate dimensions, frequency, and velocity of the heater and the resistivity are discussed and analyzed graphically. The result of the presented investigation will enable us to ensure the feasibility of the efficient design and construction of electric devices with magnetic circuits characterized by reduced heat losses.

Keywords. Eddy current, Hysteresis loss, High-frequency induction heating, Skin effect, Maxwell's equations, Ohm's law

Mathematics Subject Classification (2020). 78A25, 74A15, 74B20, 35Q61, 74A10

1. Introduction

Ferromagnetic materials have an extensive application in various electromagnetic equipment, including the magnetic circuits of motors, generators, inductors, magnetically levitated high-speed terrestrial vehicles, energy storage systems in electromagnetic fields, fusion reactors, and devices relying on electromagnetic propulsion. Compared to conventional structures that

encounter mechanical stresses, ferromagnetic structures inside strong magnetic fields are often influenced by magnetic force aroused due to the time-varying magnetic fields. The intense magnetic field causes deformation, significantly affecting material stability (Moon [15]).

Eddy-current losses have garnered significant attention from various scientific disciplines in the last several decades (Dresner [4], Sikora *et al.* [22], and Stoll [23]). Eddy currents generate power losses and subsequently thermal heating in conducting elements [25], which could negatively impact system efficiency and performance. The uneven propagation of the electric current across the surface or the skin of the current-carrying conductor is sometimes known as the "skin effect". Skin depth plays an important role in understanding the various consequences of the time-varying electromagnetic field. The dependency of skin depth on various material parameters is given by the relation:

$$\delta = \frac{1}{\sqrt{\pi f \mu \sigma}}. \tag{1}$$

The analytical formulations most typically employed in determining the heat losses due to eddy currents are described by Jassal *et al.* [7]. The harmful consequences of eddy currents in vacuum chambers have been previously reported by Kim *et al.* [9]. The thermal energy produced by eddy currents is widely used in several areas mentioned by Ebrahimi *et al.* [5], Park *et al.* [17], Rudnev *et al.* [20], and Tsopelas and Siakavellas [24] in their works. The study of the interactions of mechanical, thermal, and magnetic fields in a thermoelastic material exposed to a magnetic field is known as magneto-thermoelasticity. Magneto-thermoelasticity also covers theories like classical elasticity theory, electromagnetic theory, and heat conduction theory. The scientific notion of magneto-thermoelasticity was proposed by Chadwick [3], Knopoff [10] and later expanded upon by Kaliski and Petykiewicz [8]. Paria [16] investigated a thermo-elastic material inside a magnetic field analyzed the propagation of the plane waves and established a theoretical framework for the progress of magneto-thermoelasticity. Wilson [26] examined the propagation of magnetothermo–elastic waves in a non-rotating medium. Shen *et al.* [21] developed the suitable and most efficient heat-generating rate model to determine the temperature in induction heating using the finite element method. Roychoudhary and Banerjee [19] performed a brief study for the propagation of time-harmonic plane waves permeated by a uniform primary external magnetic field in an infinite rotating conducting, thermoelastic solid. Milošević *et al.* [12], analyzed the effect of impulsive electromagnetic radiation on temperature and elastic fields on a metallic plate using the linear theory of thermoelasticity. Milošević *et al.* [13] introduced a comparable theory for thick plates with suitable non-linear distribution. Milošević [14] analyzed the behavior of thin metallic plates exposed to electromagnetic waves using the integral transform technique. Ezzat *et al.* [6] developed a new one-dimensional mathematical model for a perfectly conducting half-space exposed to a constant magnetic field using Laplace transforms and the state-space approach. Biswas and Abo-Dahab [2] studied a three-dimensional coupled problem of electro-magneto-thermoelastic using normal mode analysis and an eigenvalue approach for a conducting solid exposed to time-dependent thermal shock. Baksi *et al.* [1] investigate a three-dimensional problem in an infinite rotating medium in the context of magneto-thermoelasticity with thermal relaxation along with heat source.

In this work, we proposed a three-dimensional mathematical model based on the analytical solution of Maxwell's equations by employing the integral transform technique. By applying

the appropriate boundary conditions the consequences of the moving high-frequency induction heater in terms of eddy current loss and hysteresis loss taking into account of skin effect are obtained analytically. Differential equations describing the various distributions of field parameters are analytically solved and obtained by employing the integral-transform technique. The effects of the time-varying electromagnetic field (and its consequences) on various field parameters of the ferromagnetic material are examined based on theoretically determined conclusions.

Interestingly, any electromagnetic device or system may be fitted with the analytic model presented in this paper. However, the primary limitation is that the conducting component needs to have a rectangular geometry. Secondly, the examined material is to be essentially made up of ferromagnetic material as we have considered the hysteresis effect which is observed only in the case of the ferromagnetic material. The most vital input is that the magnetic field to which the plate material is exposed needs to be time-varying and spatially homogenous. A numerical code is written using MATLAB® environment which allows us to derive the various graphical interpretations.

2. Governing Fundamental Equations

Electromagnetic Field

We consider the problem of a three-dimensional rectangular conducting plate that is made up of an isotropic, elastic, soft ferromagnetic material possessing a good electric conductivity occupying the space $D : 0 \leq x \leq a$, $0 \leq y \leq b$, $-h/2 \leq z \leq h/2$. Figure 1, represents the geometry of the conducting plate along with the coordinate system used.
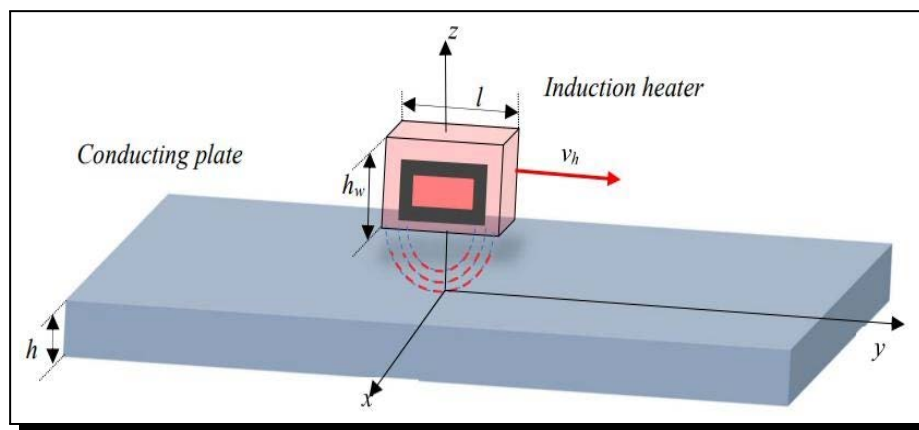
Figure 1. Conducting plate with moving frequency induction heater

The conducting rectangular plate is exposed to a linear-frequency electromagnetic heater which is moving along the y-axis of the plate geometry at constant velocity v_h. The assumptions used in the presented mathematical model are: (i) The component of magnetic induction B_x is neglected as compared to B_y due to the movement of the heater in the y-direction, (ii) the skin effect is significant, due to which the component B_z is considered negligible as compared to B_y, (iii) the presented model is rectangular and is supposed to be in 3-dimensional geometry, (iv) the magnetic material is considered to be isotropic.

The set of Maxwell's equations corresponding to the magnetic field of the plate material (neglecting charge density and displacement current) is given by:

$$\vec{\nabla} \times \vec{H} = \vec{J}, \quad \vec{\nabla} \times \vec{E} = -\frac{\partial \vec{B}}{\partial t}, \quad \vec{\nabla} \cdot \vec{E} = 0, \quad \vec{\nabla} \cdot \vec{H} = 0. \tag{2}$$

The corresponding auxiliary equations including Ohm's law are expressed as:

$$\vec{B} = \mu \vec{H}, \quad \vec{J} = \sigma(\vec{E} + \vec{u} \times \vec{B}). \tag{3}$$

The component form of the magnetic field and the induced electric field vectors are respectively given by $\vec{H} = (0, H_y, 0)$, $\vec{E} = (E_x, 0, E_z)$. The component form of the current density using equation (2), is expressed as follows:

$$(J_x, J_z) = \left(-\frac{\partial}{\partial z}, \frac{\partial}{\partial x}\right) H_y. \tag{4}$$

In the case of orthotropic conductivity, Ohm's law given by the relation $(3)_2$ is further reduced to:

$$J_x = \sigma_x E_x, \quad J_z = \sigma_z E_z, \tag{5}$$

where σ_x and σ_z represents the conductivity in respective directions.

Magnetic flux density in the components is obtained from the relation $(3)_1$ as:

$$B_y = \mu H_y. \tag{6}$$

The electric field intensity components are obtained from equations (4) and (5):

$$E_x = -\frac{1}{\sigma_x}\frac{\partial H_y}{\partial z}, \quad E_z = \frac{1}{\sigma_z}\frac{\partial H_y}{\partial x}. \tag{7}$$

Using equations (6) and (7), Faraday's law of electromagnetism i.e. relation $(2)_2$ reduces to the uncoupled equation of magnetic field as:

$$\frac{1}{\sigma_z}\frac{\partial^2 H_y}{\partial x^2} + \frac{1}{\sigma_x}\frac{\partial^2 H_y}{\partial z^2} = \mu_0 \mu_r \frac{\partial H_y}{\partial t}. \tag{8}$$

In this problem we consider the plate material to be isotropic, i.e., $\sigma_x = \sigma_z$, and $\delta_x = \delta_z = \delta = \sqrt{2/\omega\sigma\mu_0\mu_r}$. With this, equation (8) modifies to:

$$\frac{\partial^2 H_y}{\partial x^2} + \frac{\partial^2 H_y}{\partial z^2} = \frac{2}{\delta^2} H_y. \tag{9}$$

The pre-requisite boundary conditions are considered as:

$$H(x, z, t)\Big|_{x=0,a} = H_{os}, \quad H(x, z, t)\Big|_{z=0,b} = H_{os}. \tag{10}$$

Temperature field: The expressions for considered heat losses due to eddy current and the hysteresis phenomenon are given by [14]:

$$W_{eddy} = \frac{1}{2\sigma}[J_x^2 + J_z^2], \tag{11}$$

$$W_{hyste}(z, t) = k_H \mu f H_y^2. \tag{12}$$

The fundamental equations of the temperature field with prerequisite boundary and initial conditions are expressed as [13]:

$$\nabla^2 T + \frac{W_{total}}{\lambda_0} = \frac{C\rho}{\alpha}\frac{\partial T}{\partial t}, \tag{13}$$

$$T\big|_{t=0} = 0, \quad T\big|_{y=0,b} = 0, \quad \frac{\partial T}{\partial x}\Big|_{x=0,a} = 0, \quad \frac{\partial T}{\partial z}\Big|_{z=\pm h/2} = 0. \tag{14}$$

The term W_{total} represents the total heat loss and is treated as the heat source of the problem.

Elastic field: In addition to the resistive heat losses, the metallic plate is likewise subjected to the Lorentz force, $\vec{f} = \vec{J} \times \vec{B}$. With the help of equation (4) and equation (6), the Lorentz force is further deduced into component form as:

$$(f_x, f_z) = -\frac{\mu}{2} \times \left(\frac{\partial}{\partial x}(H_y)^2, \frac{\partial}{\partial z}(H_y)^2 \right). \tag{15}$$

The constitutive relations are [20]:

$$\sigma_{ij} = 2\mu e_{ij} + (\lambda e - \beta T)\delta_{ij}, e_{ij} = \frac{1}{2}(u_{i,j} + u_{j,i}). \tag{16}$$

Using equation (16), the expressions for stress fields are further reduced in component form as:

$$\sigma_{xx} = 2\mu \frac{\partial u}{\partial x} + \lambda e - \beta T, \sigma_{yy} = 2\mu \frac{\partial v}{\partial y} + \lambda e - \beta T, \tag{17}$$

$$\sigma_{zz} = 2\mu \frac{\partial w}{\partial z} + \lambda e - \beta T, \sigma_{xy} = \mu \left(\frac{\partial u}{\partial y} + \frac{\partial v}{\partial x} \right), \tag{18}$$

$$\sigma_{xz} = \mu \left(\frac{\partial u}{\partial z} + \frac{\partial w}{\partial x} \right), \sigma_{yz} = \mu \left(\frac{\partial v}{\partial z} + \frac{\partial w}{\partial y} \right), e = \frac{\partial u}{\partial x} + \frac{\partial v}{\partial y} + \frac{\partial w}{\partial z}. \tag{19}$$

The equation of motion accounting for the existence of Lorentz force is:

$$\rho \frac{\partial^2 u_i}{\partial t^2} = \frac{\partial \sigma_{ik}}{\partial x_k} + (J \times B)_i. \tag{20}$$

Further simplifying the above equations, we obtain:

$$\rho \frac{\partial^2 u}{\partial t^2} = \left[(2\mu + \lambda)\frac{\partial^2 u}{\partial x^2} + \lambda \left(\frac{\partial^2 v}{\partial x \partial y} + \frac{\partial^2 w}{\partial x \partial z} \right) - \beta \frac{\partial T}{\partial x} \right] - \frac{\mu}{2} \frac{\partial}{\partial x}(H_y)^2, \tag{21}$$

$$\rho \frac{\partial^2 v}{\partial t^2} = \left[(2\mu + \lambda)\frac{\partial^2 v}{\partial y^2} + \lambda \left(\frac{\partial^2 u}{\partial y \partial x} + \frac{\partial^2 w}{\partial y \partial z} \right) - \beta \frac{\partial T}{\partial y} \right], \tag{22}$$

$$\rho \frac{\partial^2 w}{\partial t^2} = \left[(2\mu + \lambda)\frac{\partial^2 w}{\partial z^2} + \lambda \left(\frac{\partial^2 u}{\partial z \partial x} + \frac{\partial^2 v}{\partial z \partial y} \right) - \beta \frac{\partial T}{\partial z} \right] - \frac{\mu}{2} \frac{\partial}{\partial z}(H_y)^2. \tag{23}$$

The mechanical and the initial boundary conditions are:

$$\left(\frac{\partial u}{\partial x} \right)_{x=0,a} = \left(\frac{\partial v}{\partial y} \right)_{y=0,b} = \left(\frac{\partial w}{\partial z} \right)_{z=\pm h/2} = \left(\frac{\beta}{2\mu + \lambda} \right) T, \tag{24}$$

$$(u)_{t=0} = (v)_{t=0} = (w)_{t=0} = 0. \tag{25}$$

3. Solutions

Determination of Magnetic Field. We must convert the inhomogeneous boundary conditions presented in equation (10) into homogeneous ones to determine the magnetic field expression. In light of this, we presume

$$H(x,z) = \wp(x,z) + H_{os}. \tag{26}$$

Using equation (26) in equations (9) and (10), we obtain

$$\frac{\partial^2 \wp}{\partial x^2} + \frac{\partial^2 \wp}{\partial z^2} = \frac{2}{\delta^2}(\wp + H_{os}), \tag{27}$$

$$\wp(x,z)\big|_{x=0,a} = 0, \quad \wp(x,z)\big|_{z=\pm\frac{h}{2}} = 0. \tag{28}$$

Applying the double finite Fourier sine transform [18] to equation (27) and further using it in equation (26), we obtain

$$H(x,z) = H_{os} - \Im_1 \sum_{m=1}^{\infty} \sum_{n=1}^{\infty} \xi_{mn} \sin(\zeta_m x)\sin(\zeta_m z). \tag{29}$$

The intensity of the magnetic field at any time t is expressed as:

$$H(x,z,t) = \left[H_{os} - \Im_1 \sum_{m=1}^{\infty} \sum_{n=1}^{\infty} \xi_{mn} \sin(\zeta_m x)\sin(\zeta_m z) \right] e^{\omega t}. \tag{30}$$

Current density expressions in equation (4) are modified to:

$$J_x(x,z) = a\Im_2 \left[\sum_{m=1}^{\infty} \sum_{n=1}^{\infty} n\xi_{mn} \sin(\zeta_m x)\cos(\zeta_m z) \right] e^{\omega t}, \tag{31}$$

$$J_z(x,z) = -h\Im_2 \left[\sum_{m=1}^{\infty} \sum_{n=1}^{\infty} m\xi_{mn} \cos(\zeta_m x)\sin(\zeta_m z) \right] e^{\omega t}. \tag{32}$$

Using equations (31)-(32) in equation (11) and equation (30) in equation (12), we obtain the expressions for Eddy current loss and Hysteresis loss as:

$$W_{eddy}(x,z,t) = \Im_3 \sum_{m=1}^{\infty} \sum_{n=1}^{\infty} \xi_{mn}^2 \left[\left(\frac{n}{h}\sin(\zeta_m x)\cos(\zeta_n z)\right)^2 + \left(\frac{m}{a}\cos(\zeta_m x)\sin(\zeta_n z)\right)^2 \right] e^{2\omega t}, \tag{33}$$

$$W_{hyste}(x,z,t) = k_H \mu f \left[H_{os} - \Im_1 \sum_{m=1}^{\infty} \sum_{n=1}^{\infty} \xi_{mn} \sin(\zeta_m x)\sin(\zeta_m z) \right]^2 e^{2\omega t}. \tag{34}$$

The heat source of the considered problem is the sum of the above heat losses and is mathematically expressed as:

$$W_{total}(x,z,t) = W_{eddy}(x,z,t) + W_{hyste}(x,z,t), \tag{35}$$

where $\Im_1 = \frac{8H_{os}}{ah\delta^2}$, $\Im_2 = \frac{4\mu\sigma\omega\pi H_{os}}{a^2 h^2}$, $\Im_3 = 8\sigma\left(\frac{\mu\omega\pi H_{os}}{ah}\right)^2$, $\zeta_m = \frac{m\pi}{a}$, $\zeta_n = \frac{n\pi}{h}$,

$$\Delta_{mn} = \left[\frac{((-1)^m - 1)((-1)^n - 1)}{mn\pi^2} \right], \quad \xi_{mn} = \Delta_{mn} \Big/ \left[\pi^2\left(\frac{m^2}{a^2} + \frac{n^2}{h^2}\right) + \frac{2}{\delta^2} \right].$$

Dimensionless Quantities. For the sake of simplicity, we transform all the field equations and variables in the dimensionless form and for that will use the following dimensionless variables:

$$\bar{x} = \frac{x}{b}, \quad \bar{y} = \frac{y}{b}, \quad \bar{z} = \frac{z}{b}, \quad \bar{c} = \frac{c}{b}, \quad \bar{d} = \frac{d}{b}, \quad \bar{H}_y = \frac{H_y}{H_{os}}, \quad \tau = \frac{t}{\sigma\mu b^2}, \quad (\bar{J}_x, \bar{J}_z) = \frac{b}{H_{os}}(-J_x, J_z),$$

$$\bar{W}_E = \frac{\sigma b^2 W_E}{H_{os}^2}, \quad \bar{W}_H = \frac{W_H}{k_H \mu f H_{os}^2}, \quad \bar{T} = \frac{C\rho T}{\mu H_{os}^2}, \quad (\bar{f}_x, \bar{f}_z) = \frac{b(f_x, f_z)}{\mu H_{os}^2}, \quad \bar{\sigma}_{ij} = \frac{\bar{\sigma}_{ij}}{\mu H_{os}^2/2}. \tag{36}$$

Determination of Temperature Field. The temperature field equations considering the width h_w and velocity v_h of the moving heater, in dimensionless form, are presented as (dropping the bar notation for convenience):

$$\frac{\partial^2 T}{\partial x^2} + \frac{\partial^2 T}{\partial y^2} + \frac{\partial^2 T}{\partial z^2} - \zeta_1 \frac{\partial T}{\partial \tau} = -\zeta_2 W \delta(x) \prod \left(\frac{y - v_h t}{h_w}\right)\left[H(t) - H\left(t - \frac{b}{v_h}\right)\right], \tag{37}$$

$$T\big|_{t=0} = 0, \quad T\big|_{y=0,b} = 0, \quad \frac{\partial T}{\partial x}\bigg|_{x=0,a} = 0, \quad \frac{\partial T}{\partial z}\bigg|_{z=\pm h/2} = 0. \tag{38}$$

In equation (37), the position of the heat source is described by the Dirac (δ) and the Pulsating function (Π). The heat source is assumed to be acting over the time interval $[t, t_1]$, which is mathematically expressed in terms of the Heaviside function (H).

Applying finite Fourier sine and cosine transform for y and x respectively, we obtain:

$$\left(-\Delta_{mn} + \frac{\partial^2}{\partial z^2} - \zeta_1 \partial_t\right)\widehat{\widehat{T}}(n,m) = -\frac{2h_l W_{total}}{\beta_m \lambda_0}\left[H(t) - H\left(t - \frac{b}{v_h}\right)\right]\sin(\beta_m v_h t)\sin\left(\frac{\beta_m h_w}{2}\right). \quad (39)$$

Next, we apply the finite Marchi-Fasulo integral transform [11] concerning the variable z to equation (39), to obtain:

$$[(\Delta_{mn} + a_p^2) + \zeta_1 \partial_t]\widehat{\widehat{\widehat{T}}}(n,m,p) = \left(\frac{2h_l \widehat{W}}{\beta_m \lambda_0}\right)\left[H(t) - H\left(t - \frac{b}{v_h}\right)\right]\sin(\beta_m v_h t)\sin\left(\frac{\beta_m h_w}{2}\right). \quad (40)$$

where the eigenvalues a_p's are the positive roots of the equation:

$$[\alpha_1 a \cos(ak) + \beta_1 \sin(ak)] \times [\beta_2 \cos(ak) + \alpha_2 a \sin(ak)]$$
$$= [\alpha_2 a \cos(ak) - \beta_2 \sin(ak)] \times [\beta_1 \cos(ak) - \alpha_1 a \sin(ak)], \quad (41)$$

and α_1, α_2, β_1, β_2 are the constants.

Applying the Laplace transform and its inversion to equation (40), we obtain

$$\widehat{\widehat{\widehat{T}}}(n,m,p,\tau) = \left(\frac{2h_l \widehat{W}_{total}(-1)^m}{\lambda_0 \beta_m}\right)H\left(\tau - \frac{b}{v_h}\right) \times \sin\left(\frac{\beta_m h_w}{2}\right)$$

$$\cdot\left[\left\{(\Delta_{mn} + a_p^2)\sin\left[\beta_m v_h\left(\tau - \frac{b}{v_h}\right)\right] - \beta_m v_h \cos\left[\beta_m v_h\left(\tau - \frac{b}{v_h}\right)\right]\right.\right.$$

$$\left.\left. + \beta_m v_h e^{-\left(\tau - \frac{b}{v_h}\right)(\Delta_{mn} + a_p^2)}\right\}\bigg/((\beta_m v_h)^2 + (\Delta_{mn} + a_p^2)^2)\right]. \quad (41')$$

Next, we apply the inverse finite Marchi-Fasulo integral transform followed by the inverse finite Fourier sine and cosine transform to equation (41') and obtain:

$$T(x,y,z,\tau) = \frac{8h_l W_{total}}{ab\lambda_0}H(\tau - bv_h)\sum_{n=1}^{\infty}\sum_{m=1}^{\infty}\frac{(-1)^m}{\beta_m}\sin\left(\frac{\beta_m h_w}{2}\right)\sin(\beta_m y)\cos(\alpha_n x)$$

$$\times \sum_{p=1}^{\infty}\frac{1}{\lambda_p}\left[\left\{(\Delta_{mn} + a_p^2)\sin\left[\beta_m v_h\left(\tau - \frac{b}{v_h}\right)\right] - \beta_m v_h \cos\left[\beta_m v_h\left(\tau - \frac{b}{v_h}\right)\right]\right.\right.$$

$$\left.\left. + \beta_m v_h e^{-\left(\tau - \frac{b}{v_h}\right)(\Delta_{mn} + a_p^2)}\right\}\bigg/((\beta_m v_h)^2 + (\Delta_{mn} + a_p^2)^2)\right]P_p(x). \quad (42)$$

Equation (42) represents the dimensionless temperature field.

Determination of Elastic Field. Simplifying equations (21)-(23) further and dropping the inertia term we get:

$$\frac{\partial^2 u}{\partial x^2} = \frac{\beta}{(2\mu + \lambda)}\frac{\partial T}{\partial x} + \frac{\mu}{2(2\mu + \lambda)}\frac{\partial}{\partial x}(H_y)^2, \quad (43)$$

$$\frac{\partial^2 v}{\partial y^2} = \frac{\beta}{2\mu + \lambda}\frac{\partial T}{\partial y}, \quad (44)$$

$$\frac{\partial^2 w}{\partial z^2} = \frac{\beta}{2\mu + \lambda}\frac{\partial T}{\partial z} + \frac{\mu}{2(2\mu + \lambda)}\frac{\partial}{\partial z}(H_y)^2. \quad (45)$$

Solving equations (43)-(45) further, we obtain the displacement components as:

$$u \equiv u_x = \frac{\beta}{2\mu + \lambda} \int T(x,y,z,t) dx + \frac{\mu}{2(2\mu + \lambda)} \int H(x,z,t)^2 dx, \tag{46}$$

$$v \equiv u_y = \frac{\beta}{2\mu + \lambda} \int T(x,y,z,t) dy, \tag{47}$$

$$w \equiv u_z = \frac{\beta}{2\mu + \lambda} \int T(x,y,z,t) dz + \frac{\mu}{2(2\mu + \lambda)} \int H(x,z,t)^2 dz. \tag{48}$$

The stress components in the dimensionless form are obtained by solving equations (17)-(19) further with the help of equations (46)-(48), as:

$$\sigma_{xx} = \frac{1}{2\mu + \lambda} [\mu(\mu + \lambda) H(x,z,t)^2 + 2\beta\lambda T(x,y,z,t)], \tag{49}$$

$$\sigma_{yy} = \frac{\lambda}{2\mu + \lambda} [\mu H(x,z,t)^2 + 2\beta T(x,y,z,t)], \tag{50}$$

$$\sigma_{zz} = \frac{1}{2\mu + \lambda} [\mu(\mu + \lambda) H(x,z,t)^2 + 2\beta\lambda T(x,y,z,t)], \tag{51}$$

$$\sigma_{xy} = \mu\left(\frac{\partial u}{\partial y} + \frac{\partial v}{\partial x}\right), \quad \sigma_{xz} = \mu\left(\frac{\partial u}{\partial z} + \frac{\partial w}{\partial x}\right), \quad \sigma_{yz} = \mu\left(\frac{\partial v}{\partial z} + \frac{\partial w}{\partial y}\right). \tag{52}$$

4. Numerical Results and Discussions

Soft ferromagnetic materials possess low coercivity and high permeability, which makes them highly suitable for the construction of various electromagnetic devices such as transformers that operate at minimum power losses during the operation. Magnetic Steel is one of the suitable example for soft ferromagnetic material and hence is considered for numerical assessments. The material properties considered for the steel metal to understand the numerical calculations are as defined in [13]:

$$\mu_0 = 1.26 \times 10^{-4} \text{ [H/m]}, \quad \mu = 79.3 \text{ [GPa]}, \quad \sigma = 7.7 \times 10^6 \text{ [S/m]}, \quad \nu = 0.28,$$

$$\rho = 7663 \text{ [kg/m}^3], \quad \alpha = 12 \times 10^{-6} \text{ [K}^{-1}], \quad C = 502.416 \text{ [J/kg K]}, \quad \kappa = 1.4 \times 10^{-3} \text{ [m}^2/\text{sec]},$$

$$\lambda_0 = 50 \text{ [W/mK]}.$$

Figure 2a demonstrates the relationship between skin depth and electromagnetic wave frequency for various levels of magnetic permeability. These findings indicate that the skin depth declines noticeably with increasing frequency.

Magnetic field intensity is observed to be symmetrical in both directions and it resembles a fishnet-like structure as seen in Figure 2b. Figure 3a, shows that the heat loss due to eddy current is lower at the higher resistivity values of the plate material. Figure 3b shows that the total heat loss is getting larger and larger with an increase in the frequency, meanwhile, the magnetic flux density remains constant.

(a)   **(b)**
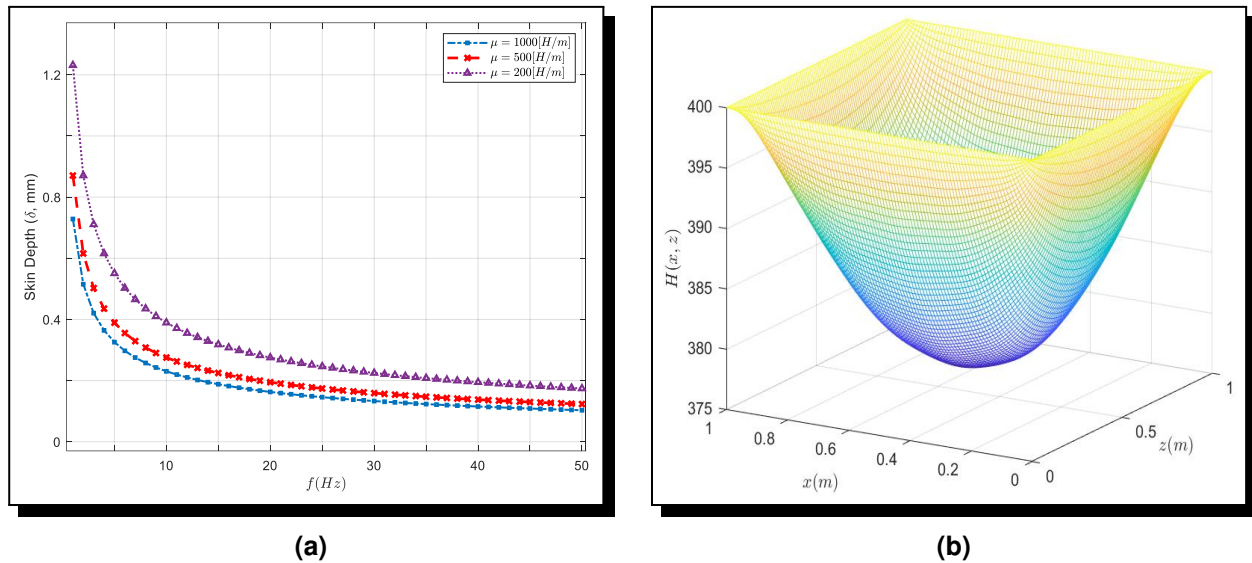
Figure 2. (a) Skin depth dependency on frequency, (b) Distribution of magnetic field intensity

(a)   **(b)**
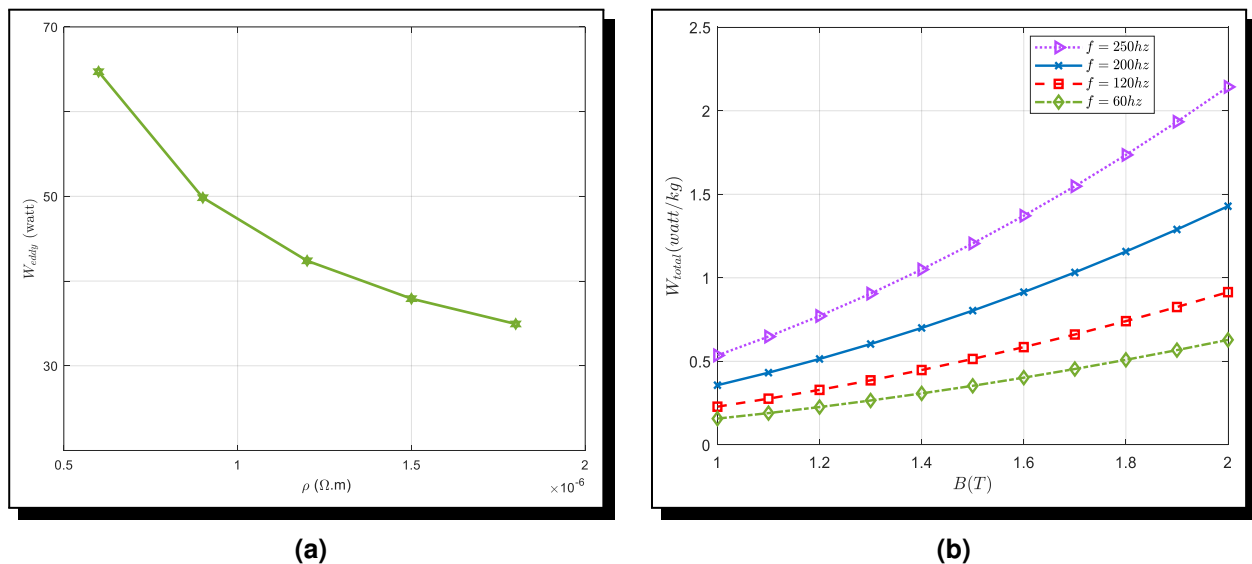
Figure 3. (a)Eddy current loss dependency on resistivity, (b) distribution of total heat loss versus flux density

Figure 4a, demonstrates variations of heat losses with frequency. We note that at low frequencies, the Hysteresis loss is a little bigger than the eddy current loss. Meanwhile, when the frequency increases over 150 Hz, the eddy current loss is significant compared to hysteresis loss. Further, when frequency increases slowly, both losses also increase. Figure 4b represents the variations in magnetic flux density (B) for steel, iron, and air with magnetic field intensity (H). We may note that variation in magnetic field density is proportional to the Magnetic field strength until it reaches a certain value from which it does not grow anymore and remains practically constant and stable while the strength of the Magnetic field continues to ascend. For Steel, the magnetic flux density increases up to 1.5 T and this point in the graph is referred to as the Magnetic Saturation. Thus, the phenomenon of Magnetic Saturation in the B-H Curve is observed. Figure 5a demonstrates the dependency of the temperature field for the various

values of the moving heater velocities. Figure 5b is a three-dimensional graph that reflects the distribution of temperature along the length and the width of the plate for various values of the thickness of the plate material. It can be observed that the temperature attains the larger values at the lower thickness and it reduces with an increase in plate thickness.
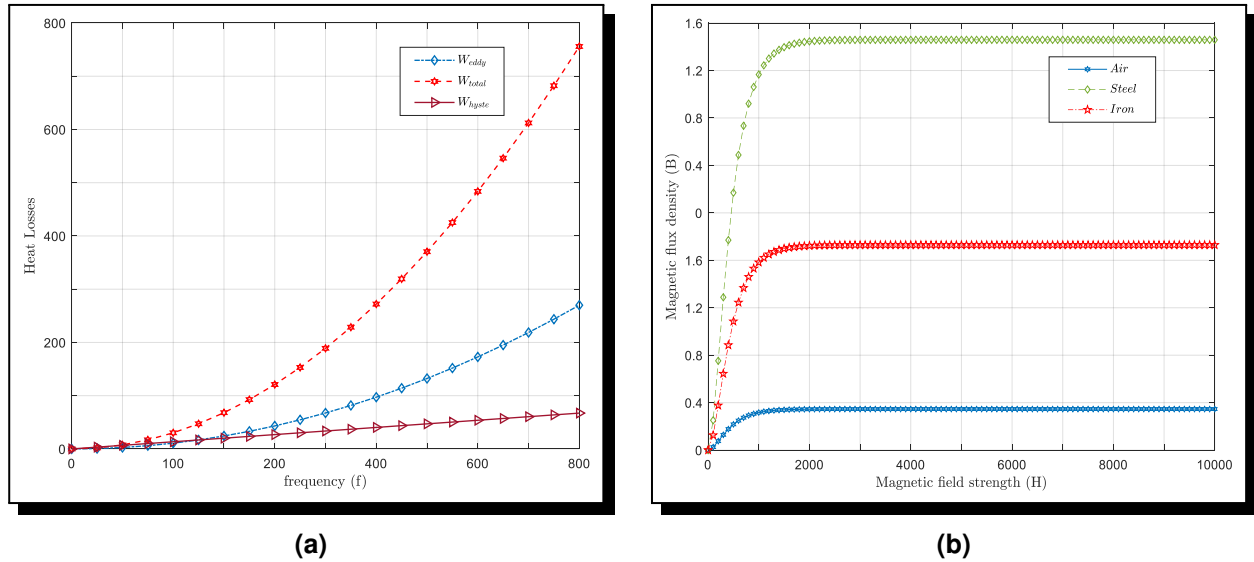

Figure 4. (a) Comparison of various heat losses, (b) B-H curve comparison for Air, steel, and Iron material

Figure 6 demonstrates the variation in the displacement along the length of the plate material at three different time values, and it can be seen that the component always begins from zero value and satisfies the corresponding boundary conditions. Also, it is concluded that the displacement component decreases as time increases. Since there is not much significant difference in the variations of the other displacement components, therefore we have ignored them in graphical analysis.
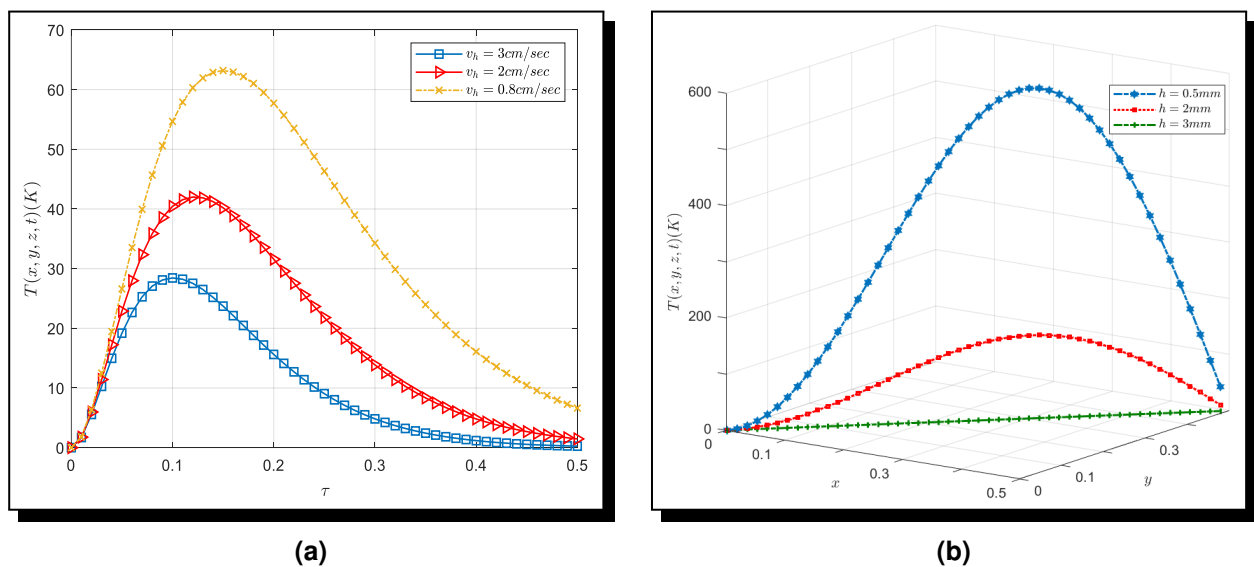
Figure 5. (a) Temperature dependence on time and heater velocity, (b) Temperature variations along the thickness of the plate
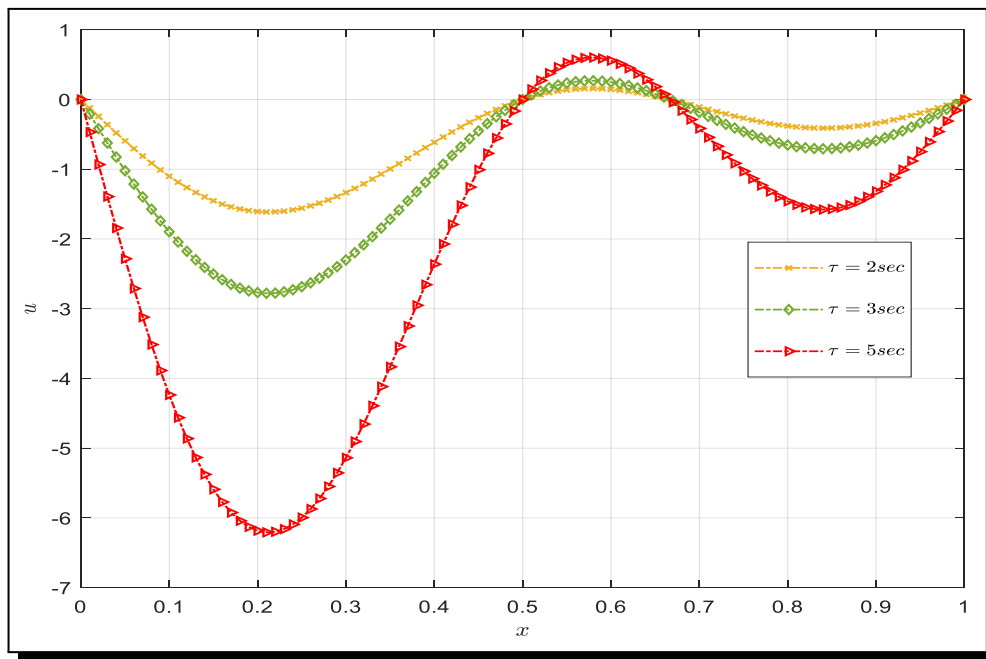
Figure 6. Displacement distribution along the length of the plate

5. Conclusion

Modeling of magneto-thermoelastic problems subjected to a high-frequency induction heater in the case of soft ferromagnetic material was successfully proposed in the present study, and the influence of frequency, heater velocity, and various parameters on the thermal and elastic fields were analyzed. The expressions for eddy current, hysteresis loss, temperature, displacement, and stress functions were obtained. The integral transform technique — a very appropriate method— was used to derive the analytical solution to the problem under consideration. Numerical results were obtained considering a special case involving a rectangular conducting plate made of magnetic steel metal, and the results were presented graphically. The conclusions are summarized below:

(i) Magnetic field shows symmetrical distribution over the plate material.

(ii) Variation in the magnetic field induces eddy current and leads to eddy current loss.

(iii) The skin depth for the considered plate material is inversely proportional to the wave frequency, hence the eddy current loss can be controlled and adjusted up to any desired depth of material by adjusting the input frequency supply.

(iv) Resistivity is the key element impacting the Eddy current loss of the plate material. Therefore by using high-resistivity materials for insulation, one can reduce the Eddy current loss to the maximum extent.

(v) Frequency has an enormous impact on both Eddy current loss and Hysteresis loss as well as on the basic characteristics of ferromagnetic materials.

(vi) The phenomenon of magnetic saturation is observed.

(vii) The temperature of the plate material is higher at the low heater velocity and it reduces as the heater velocity increases. Therefore the temperature of the plate material and the heater velocity are inversely proportional.

(viii) Temperature of the plate material decreases along the thickness of the plate which justifies the skin effect.

The present investigation will be beneficial to researchers and scientists in working on the development of new electromagnetic devices and machines that reduce heat loss and increase efficiency.

Competing Interests

The authors declare that they have no competing interests.

Authors' Contributions

All the authors contributed significantly in writing this article. The authors read and approved the final manuscript.

References

[1] A. Baksi, R. K. Bera and L. Debnath, A study of magneto-thermoelastic problems with thermal relaxation and heat sources in a three-dimensional infinite rotating elastic medium, *International Journal of Engineering Science* **43**(19-20) (2005), 1419 – 1434, DOI: 10.1016/j.ijengsci.2005.08.002.

[2] S. Biswas and S. M. Abo-Dahab, Three-dimensional thermal shock problem in magneto-thermoelastic orthotropic medium, *Journal of Solid Mechanics* **12**(3) (2020), 663 – 680, DOI: 10.22034/jsm.2020.1885944.1530.

[3] P. Chadwick, Elastic wave propagation in a magnetic field, in: *Proceedings of the International Congress of Applied Mechanics*, Brussels, Belgium, pp. 143 – 153 (1957).

[4] L. Dresner, Eddy current heating of irregularly shaped plates by slow ramped fields, Master Thesis, ORNL/TM-6968, OAK Ridge National Laboratory (ORNL), Union Carbide Corporation, USA, 1 – 44 (1979), DOI: 10.2172/5997307.

[5] B. Ebrahimi, M. B. Khamesee and F. Golnaraghi, A novel eddy current damper: Theory and experiment, *Journal of Physics D: Applied Physics* **42**(7) (2009), 075001, DOI: 10.1088/0022-3727/42/7/075001.

[6] M. A. Ezzat, A. S. El-Karamany and A. A. El-Bary, Magneto-thermoelasticity with two fractional-order heat transfer, *Journal of Association of Arab Universities for Basic and Applied Sciences* **19**(1) (2016), 70 – 79, DOI: 10.1016/j.jaubas.2014.06.009.

[7] A. Jassal, H. Polinder and J. A. Ferreira, Literature survey of eddy-current loss analysis in rotating electrical machines, *IET Electric Power Applications* **6**(9) (2012), 743 – 752, DOI: 10.1049/iet-epa.2011.0335.

[8] S. Kaliski and J. Petykiewicz, Equation of motion coupled with the field of temperature in a magnetic field involving mechanical and electrical relaxation for anisotropic bodies, *Proceedings of Vibration Problems* **4** (1959), 1 – 12.

[9] A. A. Kim, M. G. Mazarakis, V. I. Manylov, V. A. Vizir and W. A. Stygar, Energy loss due to eddy current in linear transformer driver cores, *Physical Review Special Topics – Accelerators and Beams* **13** (2010), 070401, DOI: 10.1103/physrevstab.13.070401.

[10] L. Knopoff, The interaction between elastic wave motion and a magnetic field in electrical conductors, *Journal of Geophysical Research* **60**(4) (1955), 441 – 456, DOI: 10.1029/jz060i004p00441.

[11] E. Marchi and A. Fasulo, Heat conduction in the sector of a hollow cylinder with radiations, *Atti della Reale Accademia delle scienze di Torino* **1** (1967), 373 – 382.

[12] M. V. Milošević, Temperature, strain and stress fields produced by impulsive electromagnetic radiation in the thin metallic plate, *Facta Universitatis, Series: Mechanics, Automatic Control and Robotics* **3**(12) (2002), 405 – 416, URL: http://facta.junis.ni.ac.rs/macar/macar2002/macar2002-09.pdf.

[13] M. V. Miloševic, D. Kozak, T. Maneski, N. Anđelić, B. Gaćeša and M. Stojkov, Dynamic nonlinear temperature field in a ferromagnetic plate induced by high-frequency electromagnetic waves, *Strojarstvo* **52**(2) (2010), 115 – 124, URL: https://core.ac.uk/download/pdf/14426925.pdf.

[14] M. V. Miloševic, Temperature and stress fields in thin metallic partially fixed plate induced by harmonic electromagnetic wave, *FME Transactions* **31** (2003), 49 – 54, URL: https://www.mas.bg.ac.rs/_media/istrazivanje/fme/vol31/2/vesna_milosevic-mitic.pdf.

[15] F. C. Moon, *Magneto-Solid Mechanics*, Wiley-Interscience, 436 pages (1984), DOI: 10.1115/1.3171795.

[16] G. Paria, On magneto-thermo-elastic plane waves, *Mathematical Proceedings of the Cambridge Philosophical Society* **58**(3) (1962), 527 – 531, DOI: 10.1017/s030500410003680x.

[17] I.-H. Park, I.-G. Kwak, H.-B. Lee, K.-S. Lee and S.-Y. Hahn, Optimal design of transient eddy current systems driven by a voltage source, *IEEE Transactions on Magnetics* **33**(2) (1997), 1624 – 1629, DOI: 10.1109/20.582580.

[18] F. Pasquel, Double finite Fourier sine transform and computer simulation for biharmonic equation of plate deflection, *European International Journal of Science and Technology* **8**(3) (2019), 59 – 64, URL: https://eijst.org.uk/files/articles/8.3.7.59-64.pdf.

[19] S. K. Roychoudhury and M. Banerjee, Magnetoelastic plane waves in rotating media in thermoelasticity of type II (G-N model), *International Journal of Mathematics and Mathematical Sciences* **2004**(71) (2004), 3917 – 3929, DOI: 10.1155/S0161171204404566.

[20] V. Rudnev, D. Loveless, R. Cook and M. Black, *Handbook of Induction Heating*, 1st edition, CRC Press, Boca Raton, 796 pages (2002), DOI: 10.1201/9781420028904.

[21] H. Shen, Z. Q. Yao, Y. J. Shi and J. Hu, Study on temperature field induced in high-frequency induction heating, *Acta Metallurgica Sinica* (*English Letters*) **19**(3) (2006), 190 – 196, DOI: 10.1016/S1006-7191(06)60043-4.

[22] R. Sikora, J. Purczynski, W. Lipinski and M. Gramz, Use of variational methods to the eddy current calculation in thin conducting plates, *IEEE Transactions on Magnetics* **14**(5) (1978), 383 – 385, DOI: 10.1109/tmag.1978.1059974.

[23] R. L. Stoll, *The Analysis of Eddy Currents*, Clarendon Press, Oxford, UK, (1974).

[24] N. Tsopelas and N. J. Siakavellas, Influence of some parameters on the effectiveness of induction heating, *IEEE Transactions on Magnetics* **44**(12) (2008), 4711 – 4720, DOI: 10.1109/tmag.2008.2002941.

[25] H. Vansompel, A. Yarantseva, P. Sergeant and G. Crevecoeur, An inverse thermal modeling approach for thermal parameter and loss identification in an axial flux permanent magnet machine, *IEEE Transactions on Industrial Electronics* **66**(3) (2019), 1727 – 1735, DOI: 10.1109/tie.2018.2838089.

[26] A. J. Wilson, The propagation of magneto-thermoelastic plane waves, *Mathematical Proceedings of the Cambridge Philosophical Society* **59**(2) (1963), 438 – 488, DOI: 10.1017/s0305004100037087.